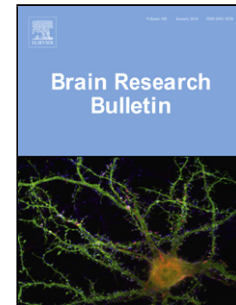


Accepted Manuscript

Title: Enrichment increases hippocampal neurogenesis independent of blood monocyte-derived microglia presence following high-dose total body irradiation

Authors: Marc J. Ruitenber, Julia Wells, Perry F. Bartlett, Alan R. Harvey, Jana Vukovic



PII: S0361-9230(17)30093-X
DOI: <http://dx.doi.org/doi:10.1016/j.brainresbull.2017.05.013>
Reference: BRB 9226

To appear in: *Brain Research Bulletin*

Received date: 20-2-2017
Revised date: 12-5-2017
Accepted date: 22-5-2017

Please cite this article as: Marc J.Ruitenber, Julia Wells, Perry F.Bartlett, Alan R.Harvey, Jana Vukovic, Enrichment increases hippocampal neurogenesis independent of blood monocyte-derived microglia presence following high-dose total body irradiation, Brain Research Bulletin <http://dx.doi.org/10.1016/j.brainresbull.2017.05.013>

This is a PDF file of an unedited manuscript that has been accepted for publication. As a service to our customers we are providing this early version of the manuscript. The manuscript will undergo copyediting, typesetting, and review of the resulting proof before it is published in its final form. Please note that during the production process errors may be discovered which could affect the content, and all legal disclaimers that apply to the journal pertain.

Title: *Enrichment increases hippocampal neurogenesis independent of blood monocyte-derived microglia presence following high-dose total body irradiation*

Running title: Neurogenesis after irradiation

Authors: Marc J Ruitenber^{a,b}, Julia Wells^c, Perry F Bartlett^b, Alan R Harvey^d, Jana Vukovic^{a,b}

^a School of Biomedical Sciences, University of Queensland, Brisbane, Queensland, Australia.

^b Queensland Brain Institute, University of Queensland, Brisbane, Queensland, Australia.

^c Telethon Kids Institute, Perth, Western Australia, Australia.

^d School of Anatomy, Physiology and Human Biology, The University of Western Australia, Perth, Western Australia, Australia

Corresponding author: Dr Jana Vukovic

Email: j.vukovic@uq.edu.au

Tel: +61 7 3345 2818

The University of Queensland (Building #81)

Brisbane QLD 4072

Australia

Highlights

- Enrichment stimulates hippocampal neurogenesis following high-dose total body irradiation.
- Exercise increases the number of microglia in the granule cell layer of the hippocampus.
- Increased microglia densities with exercise are due to local proliferation, not blood monocyte recruitment
- Monocyte-derived microglia numbers in the irradiated brain are not influenced by housing conditions
- There is no relationship between sites of monocyte infiltration and radiation-sensitive brain areas, i.e. neurogenic niches

ABSTRACT

Birth of new neurons in the hippocampus persists in the brain of adult mammals and critically underpins optimal learning and memory. The process of adult neurogenesis is significantly reduced following brain irradiation and this correlates with impaired cognitive function. In this study, we aimed to compare the long-term effects of two environmental paradigms (i.e. enriched environment and exercise) on adult neurogenesis following high-dose (10 Gy) total body irradiation. When housed in standard (sedentary) conditions, irradiated mice revealed a long-lasting (up to at least 4 months) deficit in neurogenesis in the granule cell layer of the dentate gyrus, the region that harbors the neurogenic niche. This depressive effect of total body irradiation on adult neurogenesis was partially alleviated by exposure to enriched environment but not voluntary exercise, where mice were single-housed with unlimited access to a running wheel. Exposure to voluntary exercise, but not enriched environment, did lead to significant increases in microglia density in the granule cell layer of the hippocampus; our study shows that these changes result from local microglia proliferation rather than recruitment and infiltration of circulating *Cx3cr1^{+gfp}* blood monocytes that subsequently differentiate into microglia-like cells. In summary, latent neural precursor cells remain present in the neurogenic niche of the adult hippocampus up to at least 8 weeks following high-dose total body irradiation. Environmental enrichment can partially restore the adult neurogenic process in this part of the brain following high-dose irradiation, and this was found to be independent of blood monocyte-derived microglia presence.

Keywords: Enriched environment, microglia, irradiation, bone marrow chimera, exercise, running

INTRODUCTION

Continual production of new neurons from a pool of precursor cells persists within the subgranular zone of the adult hippocampus, the brain structure that underpins learning and memory. This neurogenic process is regulated by a number of intrinsic and extrinsic factors, including hormones, neurotransmitters, growth factors, behavioural influences, drugs, and neurodegenerative diseases (for review see (1)). Reductions in the magnitude and/or rate at which new neurons are produced during ageing, inflammation, stress, social deprivation or following exposure to irradiation, correlate with deficits in hippocampal-dependent learning and memory tasks (2-5). Recent technological advances have provided direct evidence that newborn neurons are indeed important for optimal learning as their selective ablation or optogenetic silencing impairs cognitive performance (6-8).

Extensive radiation therapy is still used clinically to treat blood-related cancers, for example lymphomas, leukaemias and brain tumors. It is now known, from patient follow-up studies, that significant cognitive deficits are associated with this type of radiation treatment (for review, see 9,10). Cognitive deficits in association with irradiation are also seen in experimental animal studies, alongside dramatic reductions in adult neurogenesis (11-13). The adverse side effects of irradiation can be ameliorated through pharmacological (14) and/or immune-modulatory interventions (e.g. (12)).

To what extent the deleterious side effects of high-dose total body irradiation can be reversed through either exercise or provision of a stimulating (i.e. enriched) environment has only been addressed to a limited extent. Previous studies have clearly demonstrated, however, that introducing an animal into an enriched environment and/or allowing it to exercise can significantly boost adult neurogenesis, including following whole brain / cranial irradiation (15-18), and even improve behavioural performance (19,20). We therefore hypothesized that introducing animals to an enriched environment and/or allowing them the opportunity to

exercise voluntarily on a running wheel may also alleviate reductions in neurogenesis following total body irradiation.

Apart from its detrimental effect on neurogenesis, irradiation of the brain also leads to the influx of circulating monocytes and the differentiation of these cells into microglia (21,22). Brain microglia play an important role in fighting disease and maintaining tissue homeostasis; more recent studies have also shown, however, that microglia are also involved in a variety of other physiological processes, including the regulation of neurogenesis. In particular, recent studies have suggested that microglia provide the instructions and/or growth factors required by neural stem cells to proliferate (23-29). To what extent monocyte-derived microglia may contribute has not been investigated to date. In addition, whether or not there is specific recruitment of blood monocytes to neurogenic regions following brain irradiation due to its especially damaging effects on highly proliferative cells (i.e. neural precursors) had also remained unknown. The present study aimed to address these outstanding questions in the bone marrow (BM) chimeric mouse model.

MATERIALS AND METHODS

Animals

A total of 26 wild-type (WT) Balb/C female mice (6 weeks-of age) were used in these studies (Animal Resource Centre, Canning Vale, Western Australia), along with 5 age-matched heterozygous *Cx3cr1^{+gfp}* female mice on the same genetic background (30). In *Cx3cr1^{+gfp}* mice, one of the *Cx3cr1* alleles is disrupted by insertion of the coding sequence for eGFP; this manipulation renders the chemokine receptor itself non-functional in the mutant allele and places eGFP expression therefore under control of the *Cx3cr1* promoter. Use of the *Cx3cr1^{+gfp}* strain therefore allows all cells in the monocytic lineage to be identified via eGFP fluorescence; these mice were used as bone marrow (BM) donors during the generation of chimeric mice (see below). All mice had unlimited access to water and the same type of food throughout the experiment and were kept in the same room on a 12-h light/dark cycle. All procedures were approved by the Animal Ethics Committees of The University of Western Australia and The University of Queensland, and experiments conducted in accordance with the Australian Code of Practice for the Care and Use of Animals for Scientific Purposes.

Generation of BM chimeric mice

To ensure survival of experimental mice following high-dose total body irradiation, and to allow infiltrating monocytes / monocyte-derived microglia to be distinguished from resident brain microglia, [*Cx3cr1^{+gfp}* > WT] BM chimeric mice were generated as detailed previously (31). In brief, WT recipient mice were exposed to two doses of gamma irradiation using a 6MV photon beam from a Varian 600C linear accelerator with a field size of 40cm x 40cm. The mice were kept in standard polypropylene cages during the irradiation procedures, with the cages positioned at 1 m from the source, i.e. the depth of dose maximum of the beam. The total dose of 10 Gy was delivered in two 5 Gy fractions delivered 14 h apart, with the dose

rate being 2.5 Gy/min. The method of dose calculation for the irradiation procedure was the same as that used for the treatment of radiotherapy patients. Irradiated WT recipient mice were then given a BM transplant from *Cx3cr1^{+/gfp}* donor mice via the lateral tail to rescue their hematopoietic system (3-4 h after the second dose of irradiation); for each irradiated recipient animal, 5×10^6 donor BM cells were injected via lateral tail vein. Mice were left to recuperate for 8 weeks, with 6-8 mice housed socially in standard cages.

Housing conditions and BrdU injections

To examine the effect of delayed exposure to enriched environment and exercise on hippocampal neurogenesis and microglia (i.e. 8 weeks after high-dose irradiation and BM transplantation), mice were randomly selected and transferred to one of three housing conditions: One group of chimeric animals (n=8) was placed together in standard housing, that is, a cage with nesting materials only. Mice in the second group (n=8) were co-housed under environmentally enriched conditions. The third group of animals (n=6) was housed solitary in cages that contained a running wheel with an odometer attached. A fourth group of mice consisted of age-matched, non-irradiated wild-type controls (n=4), which was also maintained in standard housing. The specific experimental design is illustrated in **Figure 1A**.

To maintain a high level of novelty for animals housed in enriched environment, we slowly expanded the cage system as we hypothesized that this would maximally stimulate neurogenesis; the maze attached to the standard housing was expanded and the complexity increased on a weekly basis. Specifically, novel objects and accessible pathways within the maze were added on a weekly basis. In week 1, the enriched environment involved only two cages (on one level), which were connected by tubing; one cage had a food source and a nesting area, the other cage had a running wheel. In each subsequent week, the setup of the enriched environment was altered and expanded through the addition of more tubing and

mazes. Overall complexity of the enriched environment towards the end of the experiment involved four levels of accessible areas for the mice. Location of food sources and the orientation of the maze were re-located on a weekly basis, as were nesting boxes and other objects. Mice were also provided with opportunities for food reward via almost vertical climbs. The initial cage system is shown in **Figure 1B**; the expanded environment at the study endpoint is shown in **Figure 1C**.

To compare cell proliferation and neural precursor cell activity within the sub-granular layer of the adult hippocampus between housing conditions, all mice were intraperitoneally injected with bromodeoxyuridine (BrdU; 100 mg/kg body weight); BrdU administration was initiated following a 6-week exposure period to the various housing conditions (i.e. 14 weeks following irradiation), once daily for 5 consecutive days while the animals remained in their respective environments. BrdU injections were always given 2 h after commencement of the light cycle to minimize the influence of circadian variations in neurogenesis between conditions (32). All mice were euthanized one week after the last BrdU injection (see below).

Tissue collection and processing

Mice were anaesthetized with sodium pentobarbital (50 mg/kg) and transcardially perfused using saline solution, followed by 4% paraformaldehyde in 100 mM phosphate buffer (pH 7.4). Brains were dissected out, post-fixed overnight at 4°C, and equilibrated in phosphate buffered 10% and 30% sucrose for cryoprotection. A coronal cut was made just rostral to the cerebellum, after which the cut aspect of the brain was placed onto a piece of sterile cardboard, followed by snap-freezing in dry-ice cooled isopentane and storage at -80°C until further processing. Coronal sections (50 µm) were cut using a cryostat and then transferred into 48-well plates containing cryoprotectant (300 g sucrose, 300 ml ethylene glycol, 1.59 g sodium phosphate monobasic, 5.47 g sodium phosphate dibasic, 9.0 g sodium chloride, 10 g

polyvinylpyrrolidone in 1 l of deionized water, pH 7.4); this solution preserves both the integrity and antigenicity of the tissue when stored at -20°C.

Immunostaining

Series of 1 in 6 sections were selected for free-floating peroxidase-based immunohistochemistry in order to visualize proliferating cells (BrdU^{POS} cells), newborn neurons (doublecortin-positive; DCX^{POS} cells), total CNS microglia (Iba1^{POS} cells), and donor BM-derived microglia (GFP^{POS} cells). Of these series, an average of 8 to 10 sections per brain contained the hippocampus. Sections were removed from cryoprotectant solution and thoroughly washed three times, 1 h per wash, in phosphate-buffered saline (PBS; pH 7.4; 1.5 ml/well) before being left overnight in PBS at 4°C. The following day, sections were washed an additional three times in PBS at room temperature (RT); all washing steps were performed on an oscillating rocker.

Endogenous peroxidase activity was blocked by incubation in quenching solution, i.e. 10% methanol and 0.6% H₂O₂ in PBS, for 30 min at RT. For anti-BrdU staining an additional DNA denaturation step preceded the quenching step, which involved immersion of the sections in 2N HCl for 45 min at 37°C. Sections were then washed again, after which blocking solution containing 2% bovine serum albumin (Sigma) and 0.2% Triton X-100 in PBS was applied for 1 h at RT; blocking solution was also used as an antibody diluent in all subsequent incubation steps. Rabbit anti-GFP antibody (1:1000, Vector Laboratories) was used to stain for donor BM-derived microglia/macrophages, rabbit anti-mouse Iba1 (1:500, Wako Chemical Industries) was used for general microglia staining, rat anti-mouse BrdU (1:1000, Serotec Laboratories) was used to visualize proliferating cells and rabbit-anti mouse DCX (1:500, Abcam) was used to stain for newborn neurons. All primary antibodies were applied overnight at 4°C. The following day, sections were washed extensively (3 x 10 min in

PBS) before being incubated for 90 min at RT with either biotinylated goat anti-rabbit (1:400, Vector Laboratories) or biotinylated donkey anti-rat (1:200, Jackson Immuno Research Laboratories) secondary antibodies. After another round of washings, sections were incubated with an avidin-biotin-peroxidase complex (1:200, Vectastain Elite ABC; Vector Laboratories) for 1 h at RT. The sections were then incubated in 3'-diamino-benzidine (DAB; Sigma) until the brown precipitate that develops as part of the enzymatic reaction with peroxidase became clearly visible under a light microscope (~ 5 min). The sections were then immersed in ddH₂O to stop the reaction, washed in PBS, mounted on Superfrost™ Plus glass slides and then left overnight to dry. The following day, slides were immersed in 4% paraformaldehyde for 30 to 60 min, after which the sections were counterstained for Nissl substance (thionine or cresyl violet) and then dehydrated and coverslipped.

To confirm that GFP^{pos} cells were indeed donor BM-derived brain microglia and/or perivascular macrophages and/or brain microglia, a separate set of sections was double-labelled with a mixture of GFP and Iba1 antibodies. Sections were left overnight at 4°C immersed in antibody diluent containing monoclonal mouse anti-GFP (1:200, Vector Laboratories) and rabbit anti mouse-Iba1 (1:250). The following day, sections were washed before being incubated for 1 h at RT in goat anti-mouse Alexa Fluor 488 (1:200, Invitrogen) and goat anti-rabbit Alexa Fluor 546 (1:200, Invitrogen).

To distinguish perivascular macrophages from donor BM-derived microglia in the brain parenchyma, sections were double-labelled with GFP and a pan-laminin antibody, which stains vascular structures. GFP^{pos} cells with a bipolar morphology were always found in close association with microvessels, confirming them to be typical perivascular macrophages; these cells were excluded from quantitative analysis as our primary aim was to study donor BM-derived microglia in the irradiated host brain. The primary antibodies used here were rabbit anti-mouse GFP (1:200, Vector Laboratories) and monoclonal mouse anti-

pan-laminin (1:400; Sigma). Secondary antibodies used were goat anti-rabbit Alexa Fluor 488 (1:200, Invitrogen) and goat anti-mouse Alexa Fluor 546 (1:200, Invitrogen).

After incubation, sections were washed, mounted on to Superfrost™ Plus slides and left to dry for 10 min. Slides were then coverslipped in fluorescence mounting medium (Dako) containing Hoechst 33342 nuclear dye. Images were captured using a Biorad MRC 1000/1024 UV confocal microscope.

Microscopic analysis and quantification

Immunohistochemically stained slides were digitized using a slide scanner (Scanscope XT system, Aperio Technologies) at 40x digital zoom. Scanned images were presented as a single plane of focus, so a modified optical fractionator method with Abercrombie correction factor was used to estimate the total number of BrdU-, DCX-, GFP- and Iba1-positive cells within the hippocampus. Stained (i.e. BrdU⁺, DCX⁺, Iba-1⁺ or GFP⁺) cells were counted in the discrete layers of the hippocampus along its rostral-caudal axis, -0.94 to -4.04 mm from Bregma using an extensive sampling scheme. Every sixth section was counted using a fractionator method (33), with counts obtained from 8 to 10 sections per mouse; sampled sections were 300 µm apart. The dorsal (anterior) portion of the dentate gyrus starts at -0.94 mm from Bregma while the ventral (posterior) aspect of the dentate gyrus only starts at -2.46 mm from Bregma (34). Random sample comparisons were made for 4 animals between the GFP^{pos} cell counts derived from scanned images as compared to those obtained through manual counting using a light microscope (Leica) with a 40x objective. Both methods produced similar cell counts (data not shown), validating the use of images from the Aperio scanner for quantification.

BrdU-labelled cells were only included in the counts if they displayed a darkly stained nucleus, which was spherical in shape, and for GFP^{pos} cells if they were present within the

parenchyma, that is they were not associated with cells within (or lining) blood vessels and/or meningeal structures (**Figure 5A,B**). The total analysed image area was not significantly different between mice in the various experimental groups. In all instances, the individual performing the counts was blinded to the experimental conditions.

Statistical analysis

Data sets are presented as dot plots or as mean \pm SEM, and were examined for statistical significance using either a one- or 2-way repeated measures ANOVA followed by Tukey's *post-hoc*. Data sets were considered significantly different from each other at $p < 0.05$ and a statistical power level of 0.8 or greater.

RESULTS

Enrichment augments hippocampal neurogenesis following total body irradiation

To assess the long-term impact of high-dose irradiation treatment on adult neurogenesis in the dentate gyrus of the hippocampus, animals were injected with BrdU over 5 days and then sacrificed 7 days after the last injection (**Figure 1A**). A cohort of non-irradiated wild-type mice ($n=4$), which was age-matched and kept for 16 weeks in the same standard housing as their irradiated sedentary counterparts ($n=7$), was included for reference. Numerous BrdU^{pos} cells were found in the granule cell layer of 22-week-old non-irradiated wild-type mice that were kept in standard housing (**Figure 2A**). Note that age-matched, irradiated mice, which were maintained under the same standard housing conditions, showed significantly fewer BrdU^{pos} cells in the granule cell layer (**Figure 2B**). Quantitative counts confirmed these visual observations and revealed a 78% decrease in BrdU^{pos} cell numbers within the granule cell layer of irradiated mice compared to non-irradiated, sedentary controls (Non-irradiated: 1212 ± 95 cells vs. Sedentary: 272 ± 21 cells; $p < 0.0001$; **Figure 2E**). This adverse effect of high-dose total body irradiation was partially mediated in mice that were

housed in environmentally enriched conditions (**Figure 2C**), whereas the running paradigm did not appear to have any beneficial effect (**Figure 2D**). Quantitative counts again confirmed these observations; specifically, mice that lived in environmentally enriched housing were found to have a significantly greater number of BrdU^{POS} cells in the granule cell layer of the dentate gyrus compared to both irradiated, sedentary animals and those housed with running wheels (Env Enrichment: 625 ± 75 cells vs Sedentary: 272 ± 21 cells $p < 0.001$; Env Enrichment: 625 ± 75 cells vs Running wheel: 313 ± 17 cells; $p < 0.005$; **Figure 2E**).

In addition to BrdU^{POS} cell numbers, there was also a 95% reduction in the presence of DCX^{POS} cells (i.e. immature neurons) in the granule cell layer of the hippocampus at 16 weeks after high-dose total body irradiation (Non-irradiated: 1265 ± 22 vs Sedentary: 64 ± 10 cells; $p < 0.0001$; **Figure 2F**), illustrating the long-term deleterious effects of such treatment on neurogenesis in the dentate gyrus. Consistent with the increase in BrdU^{POS} cell numbers in mice that were living under environmentally enriched conditions, this group also had a greater number of DCX^{POS} cells in the granule cell layer of the dentate gyrus compared to their irradiated counterparts that were housed under sedentary conditions (Env. Enrichment: 322 ± 47 cells vs Sedentary: 64 ± 10 cells; $p < 0.01$) or with access to a running wheel (Env. Enrichment: 322 ± 47 vs Running Wheel: 155 ± 33 cells; $p < 0.05$; **Figure 2F**). It should be noted here that we were only able to analyze DCX^{POS} cell numbers from just two mice that were housed under environmentally enriched conditions due to limited tissue availability. Whilst we are cognizant of this limitation, extensive statistical modeling has shown that unequal and very small (even down to $n=2$) can still yield acceptable power under the following conditions: 1) a large effect size (i.e. an > 5 -fold difference between groups – as observed here), and 2) that the findings are in general agreement with existing relevant literature in the field (35). Wheel running for an 8-week period did not lead to a statistically significant increase in DCX^{POS} cell numbers in our experimental paradigm compared to

sedentary controls (Running Wheel: 155 ± 33 cells vs Sedentary: 64 ± 10 cells; $p=0.16$) despite the fact that, on average, ‘runner’ mice ran 16.04 km/week (ranging from 10.43 km to 19.99 km per week); the distance covered by individual animals also had no bearing on neurogenesis. It should be noted, however, that these mice were housed solitary and the distance run appears to be less than what has been previously reported in literature (i.e. 28-84 km/week; 26, 60, 61). Overall, mice that were housed with environmental enrichment displayed a 50% increase in BrdU^{POS} cell numbers compared to non-irradiated controls. The increase in the DCX^{POS} cell numbers under environmentally enriched conditions accounted for ~20% of the total number of DCX^{POS} cells seen in age-matched non-irradiated animals (**Figure 2F**).

Exercise results in an increased number of microglia in the granule cell layer

In addition to examining how different housing conditions influenced neurogenesis in the hippocampus following exposure to high-dose irradiation, we also examined whether the different housing environments had an impact on the total number of microglia in the granule cell layer and the dentate gyrus. Iba1 staining revealed a relatively uniform distribution of ramified microglia throughout the dentate gyrus of all animals, regardless of housing conditions (**Figure 3A & B**). Quantitative counts did, however, reveal a significant increase in Iba1^{POS} cell numbers within the granule cell layer of runner mice compared to (irradiated) sedentary mice (Running Wheel: 2055 ± 240 cells vs Sedentary: 1232 ± 173 ; $p<0.05$; **Figure 3C**); enriched environment did not increase the number of Iba1^{POS} cells in the granule cell layer compared to their sedentary counterparts (Env. Enrichment: 1702 ± 158 cells vs Sedentary: 1232 ± 173 ; $p=0.24$). Similar trends were seen for total Iba1^{POS} cell numbers in the entire dentate gyrus (**Figure 3D**). In summary, the present data show that voluntary wheel running most significantly affected microglia proliferation in the granule cell layer of the

dentate gyrus following total body irradiation, as evidenced by the increase in total Iba1^{POS} cell numbers.

Monocyte recruitment to the irradiated brain is not associated with increased adult neurogenesis under environmentally enriched conditions

Having shown that enriched environment increases adult neurogenesis in the granule cell layer, we next examined whether this increase also involved recruitment of circulating blood monocytes (blood monocyte-derived microglia) into this region. Since we used *Cx3cr1^{+/-gfp}* BM transplants to ensure mouse survival following total body irradiation, infiltrating microglia-like cells of peripheral origin could be distinguished from host microglia on the basis of GFP expression (**Figure 4A & B**). We observed that all ramified GFP^{POS} cells within the hippocampus of chimeric mice were positive for the pan-microglia marker Iba1. Double immunofluorescence staining for GFP and laminin confirmed that these ramified cells were indeed newly differentiated microglia of donor bone marrow origin, as opposed to perivascular macrophages that were mostly bipolar in morphology and closely associated with basement membrane structures of blood vessels (**Figure 4A & B**). This clear morphological distinction was used in stereology protocols to estimate microglia numbers in the hippocampus after immunohistochemical staining for GFP or Iba-1.

BM-derived microglia-like cells at the study endpoint were predominately found in the more ventral aspects of the cortex (**Figure 4C**). Relatively few GFP^{POS} cells were encountered in the more dorsal aspects of the brain after total body irradiation, though small clusters of GFP^{POS} cells did appear on occasion within the cortical parenchyma here. Substantial numbers of GFP^{POS} cells were observed within meningeal structures surrounding the brain, regardless of anatomical location. Consistent with the neocortical observations, only few GFP^{POS} cells were observed in the dorsal (anterior) dentate gyrus of the hippocampus

(**Figure 4D**), while a much greater number of GFP^{POS} cells was observed in the ventral-posterior aspects of the dentate gyrus (**Figure 4E**). Quantitative assessment of GFP^{POS} cell numbers in the granule cell layer of dentate gyrus and also other parts of the hippocampus, as specified in **Figure 4F,G**, revealed no statistically significant differences ($p>0.05$, repeated measures two-way ANOVA) in the number of GFP^{POS} cells between the chimeric sedentary mice (standard housing; $n=5$), those housed in an enriched environment ($n=5$), and those with access to just running wheel ($n=5$). This finding indicates that the environment in which the animal is housed 8 weeks after total body irradiation does not have an impact on the number of donor BM-derived (i.e. GFP^{POS}) microglia-like cells in this part of the brain. As the GFP^{POS} donor BM-derived microglia comprised only a small proportion (<1% in the dorsal and 7% in the ventral granule cell layer) of the total Iba1^{POS} microglia within the granule cell layer, the significant increase in Iba1^{POS} cell numbers in the granule cell layer following running (see **Figure 3D**) thus mostly results from local microglia proliferation.

Having established that there was no overall change in the total number of donor BM-derived microglia, we examined the relative distribution of these cells with regards to the neurogenic regions of the hippocampus. GFP^{POS} donor BM-derived microglia-like cells were most plentiful in the ventral (posterior) subregion of the granule cell layer of the hippocampal dentate gyrus with only few cells detected septally (**Figure 5 C-E**). Indeed, a significant change ($p<0.0001$; repeated measures two-way ANOVA) was observed for the number of infiltrating GFP^{POS} in the dorsal vs ventral hippocampus (Hip), dentate gyrus (DG), granule cell layer of the dentate gyrus (GrDG), polymorph layer of the dentate gyrus (PoDG), pyramidal cell layer of the dentate gyrus (PyDG) and oriens layer of the hippocampus (OrDG) (**Figure 5 F,G**). In contrast, BrdU^{POS} cells were significantly more abundant in the more dorsal (i.e anterior) aspect of the granule cell layer for all chimeric mice regardless of housing conditions, which is consistent with there only being a very limited amount of neurogenic

niche (i.e. granule cell layer) present within the ventral aspect of the dentate gyrus.

Recruitment and/or presence of blood monocyte-derived microglia in the hippocampus thus did not specifically link to the neurogenic niche, i.e. the area most sensitive to irradiation-induced cell death.

DISCUSSION

The present study found that high-dose total body irradiation had a long-term detrimental effect on the proliferative capacity of cells within the hippocampus; exposure to an enriched environment partially reversed this effect, but solitary wheel running did not. Compared to sedentary animals, total microglia numbers were higher in the granule cell layer of mice exposed to enriched environment but particularly so following voluntary wheel running. There was no relationship between the presence of bone marrow-derived microglia and areas of neural precursor cell proliferation within the granule cell layer of the dentate gyrus following total body irradiation.

Environmental enrichment alleviates the depression of hippocampal neurogenesis following high-dose irradiation

Irradiation exerts a direct suppressive effect on highly proliferative stem/progenitor cells in the brain and also negatively alters the signaling in the local microenvironment that normally underpins neurogenesis (36). Comparisons with age-matched non-irradiated WT mice indeed revealed the significant and long-term detrimental effect of irradiation on proliferative capacity in the dentate gyrus of sedentary bone marrow chimeric mice, for at least 16 weeks after exposure to high-dose total body irradiation (2x 5 Gy, delivered 14 h apart). These observations are also consistent with previous studies showing that the detrimental effects of cranial irradiation on hippocampal neurogenesis are dose-dependent, with dosages of 5-6 and

10 Gy (but not 2 or 4 Gy) resulting in reduced levels of cell proliferation at least 17 weeks (13, 37-41).

The positive influence of voluntary physical activity (20, 42) and enriched environments (19) on cell proliferation in the neurogenic niches of the adult brain is well established. In this study, we found that environmental enrichment is particularly effective in promoting proliferative capacity in the dentate gyrus following a high (sub-lethal) dose of total body irradiation. This significant increase in the number of proliferating cells was accompanied by an increased presence of doublecortin-positive newborn neurons within the granule cell layer of the hippocampus compared to sedentary animals. Previous work by Fan *et al.* (43) reported that gerbils receiving a 10 Gy dose of irradiation, which was targeted to the brain, also showed enhanced neurogenesis after exposure to environmental enrichment 4-weeks after a 10 Gy dose of irradiation. The present findings show that hippocampal neurogenesis can be stimulated, at least in the rodent, for up to at least 8 weeks after total body irradiation. Interestingly, in a mouse model with a fractionated 15 Gy dose of irradiation, enriched housing for 15 weeks after an 8-week rest period was reported to have no effect on irradiation-induced reductions in cell proliferation within the dentate gyrus (44). This finding could indicate an upper threshold after which the neurogenic capacity of the SGZ can no longer recover from irradiation and/or a critical time period (i.e. less than 8 weeks), in which intervention strategies must be initiated.

The finding that voluntary wheel running did not significantly increase cell proliferation within the neurogenic region of the hippocampus appears, at least at first sight, somewhat contrary to published reports (15, 45-47). Reasons for this seeming discrepancy may include social isolation (i.e. solitary housing) and/or the duration of exercise. Specifically, in most other studies, mice or rats were housed socially in small groups with shared access to a running wheel, and this is normally associated with increased cell proliferation in the

hippocampus compared to controls housed in standard caging (20, 42). In the present study, animals with running wheels were housed individually in order to ascertain the distance run by individual mice per day. This experimental set up may, however, have contributed to lack of an exercise effect in these mice. Specifically, a previous study by Stranahan *et al.* (48) reported that social isolation of male rats retarded the effect of voluntary exercise (wheel running) on increasing hippocampal neurogenesis; this was coincided by increased corticosterone levels as an indicator of heightened stress levels. Leasure and Decker (49) reported that female rats were also sensitive to the depressive effects of social deprivation (i.e. solitary housing) with regards to exercise-induced neurogenesis in the hippocampus. The time for which animals were allowed to exercise (i.e., 8 weeks) may also have contributed to the lack of a rescue effect on hippocampal neurogenesis following irradiation in the runner group (61).

Microglia density in the granule cell layer is not altered by monocyte recruitment

We also explored whether monocyte recruitment to the brain following high-dose total body irradiation contributes significantly to increases in microglia density within the granule cell layer of the hippocampus, which reportedly occur following housing in environmentally enriched (i.e. neurogenic) conditions and/or with access to a running wheel. Specifically, previous studies by Ziv *et al.* (24) and Williamson *et al.* (51) reported an increase in number of microglia in the dentate gyrus of (non-irradiated) rats after exposure to environmental enrichment. In the present study, we did not observe a statistically significant increase in the number of microglia under our own enriched environment paradigm. The number of Iba1^{POS} microglia in the granule cell layer of the hippocampus was, however, significantly increased after wheel running. Thus, while the enriched environment paradigm appeared most effective

in stimulating proliferation of neural precursors, the exercise regimen appeared to have the most potent effect on microglia proliferation.

Taking advantage of the fact that high-dose total body irradiation requires a bone marrow transplant to ensure survival, we were able to explore whether changes in microglia density resulted from local proliferation of CNS resident microglia, recruitment of blood monocytes, or both. As we did not observe significant differences in the number of donor BM-derived (i.e. GFP^{POS}) microglia within the granule cell layer of the hippocampus between the experimental/housing conditions (along with the fact that their overall numbers were relatively small), increases in the density of Iba1^{POS} microglia due to e.g. voluntary wheel running must be mostly due to local proliferation (52).

New monocyte-derived microglia have previously been reported throughout the CNS in various neurogenic and non-neurogenic locations using a similar chimeric animal model (53), and their presence relies on brain irradiation as a conditioning/recruiting factor (21, 22). The signals that direct recruitment of monocytes towards specific (inflamed) brain regions involve the chemokine receptor CCR2 and its ligand, CCL2 (54, 55). GFP^{POS} donor BM-derived microglia were primarily present in the ventral (i.e. more posterior) portion of the hippocampus. Similar to Morganti et al. (56), some recruitment and differentiation of donor bone marrow-derived cells into microglia was observed in the dorsal hippocampus but these were far fewer in numbers compared to the ventral hippocampus. This differential pattern of donor BM-derived microglia for different parts of the hippocampus (as well as other brain regions) has been consistently observed by us in multiple independent experiments, with survival times of up to 6 months post-chimerisation (unpublished observations). These differences in anatomical distribution, which resemble the pattern of YFP^{POS} cells in the brains of CD11c-YFP reporter mice (57), may have resulted from region-specific differences in local inflammation and/or blood-brain barrier integrity following irradiation. Alternatively, and not

mutually exclusive, microglia proliferation rates, including those of donor BM origins, may vary between regions. Regardless, the present study shows that donor BM-derived cells do not appear to be specifically recruited to neurogenic areas in which cell death after total body irradiation would have been higher due to the presence of proliferating (i.e. radiosensitive) precursor cells as no positive correlation was observed between BrdU- and GFP-positive cell numbers.

In summary, we demonstrate that neural stem/progenitor cells still exist within the neurogenic niche of the hippocampus following high-dose total body irradiation, and that impairments in neurogenesis under these conditions can be partially alleviated through environmental enrichment. Given that hippocampal neurogenesis is now known to occur in humans throughout life (58), these findings may be of particular significance to patients who undergo total body irradiation and/or high-dose chemotherapy for the treatment of various malignancies, and in which cognitive deficits have been reported (9, 10), alongside profoundly inhibited hippocampal neurogenesis (59).

ACKNOWLEDGMENTS

We thank Karen Waldock and Peter Lanzon for their help with mouse irradiation protocols, and the animal care facility staff for breeding and maintaining the animals used in this study.

We also thank Ashley Cooper and Rowan Tweedale for editorial assistance. J.V. is the recipient of an Australian Research Council Discovery Early Career Research Award (DE150101578).

REFERENCES

1. Vukovic J, Blackmore DG, Jhaveri D, Bartlett PF. Activation of neural precursors in the adult neurogenic niches. *Neurochem Int* 2011; 59:341-6.
2. Cinini SM, Barnabe GF, Galvão-Coelho N, de Medeiros MA, Perez-Mendes P, Sousa MB, et al. Social isolation disrupts hippocampal neurogenesis in young non-human primates. *Front Neurosci* 2014; 8:100-7.
3. Naninck EF, Hoeijmakers L, Kakava-Georgiadou N, Meesters A, Lazic SE, Lucassen PJ, et al. Chronic early life stress alters developmental and adult neurogenesis and impairs cognitive function in mice. *Hippocampus* 2015; 25:309-28.
4. Ryan SM, Nolan YM. Neuroinflammation negatively affects adult hippocampal neurogenesis and cognition: can exercise compensate? *Neurosci Biobehav Rev* 2015; 61:121-31.
5. Son Y, Yang M, Wang H, Moon C. Hippocampal dysfunctions caused by cranial irradiation: a review of the experimental evidence. *Brain Behav Immun* 2015; 45:287-96.
6. Gu Y, Arruda-Carvalho M, Wang J, Janoschka SR, Josselyn SA, Frankland PW, et al. Optical controlling reveals time-dependent roles for adult-born dentate granule cells. *Nat Neurosci* 2012; 15:1700-6.

7. Vukovic J, Borlikova GG, Ruitenbergh MJ, Robinson GJ, Sullivan RK, Walker TL, et al. Immature doublecortin-positive hippocampal neurons are important for learning but not for remembering. *J Neurosci* 2013; 33:6603-13.
8. Garrett L, Zhang J, Zimprich A, Niedermeier KM, Fuchs H, Gailus-Durner V, et al. Conditional Reduction of Adult Born Doublecortin-Positive Neurons Reversibly Impairs Selective Behaviors. *Front Behav Neurosci* 2015; 9:302.
9. Monje M. Cranial radiation therapy and damage to hippocampal neurogenesis. *Dev Disabil Res Rev* 2008; 14:238-42.
10. Padovani L, Andre N, Constine LS, Muracciole X. Neurocognitive function after radiotherapy for paediatric brain tumours. *Nat Rev Neurol* 2012; 8:578-88.
11. Kalm M, Karlsson N, Nilsson MK, Blomgren K. Loss of hippocampal neurogenesis, increased novelty-induced activity, decreased home cage activity, and impaired reversal learning one year after irradiation of the young mouse brain. *Exp Neurol* 2013; 247:402-9.
12. Monje ML, Toda H, Palmer TD. Inflammatory blockade restores adult hippocampal neurogenesis. *Science* 2003; 302:1760-5.
13. Rola R, Raber J, Rizk A, Otsuka S, VandenBerg SR, Morhardt DR, et al. Radiation-induced impairment of hippocampal neurogenesis is associated with cognitive deficits in young mice. *Exp Neurology* 2004; 188:316-30.
14. Manda K, Reiter RJ. Melatonin maintains adult hippocampal neurogenesis and cognitive functions after irradiation. *Prog Neurobiol* 2010; 90:60-8.
15. Naylor AS, Bull C, Nilsson MK, Zhu C, Bjork-Eriksson T, Eriksson PS, et al. Voluntary running rescues adult hippocampal neurogenesis after irradiation of the young mouse brain. *Proc Natl Acad Sci USA* 2008; 105:14632-7.

16. Blackmore DG, Golmohammadi MG, Large B, Waters MJ, Rietze RL. Exercise increases neural stem cell number in a growth hormone-dependent manner, augmenting the regenerative response in aged mice. *Stem Cells* 2009; 27:2044-52.
17. Wong-Goodrich SJ, Pfau ML, Flores CT, Fraser JA, Williams CL, Jones LW. Voluntary running prevents progressive memory decline and increases adult hippocampal neurogenesis and growth factor expression after whole-brain irradiation. *Cancer Res* 2010; 70:9329-38.
18. Blackmore DG, Vukovic J, Waters MJ, Bartlett PF. GH mediates exercise-dependent activation of SVZ neural precursor cells in aged mice. *PloS One* 2012; 7:e49912.
19. Kempermann G, Kuhn HG, Gage FH. More hippocampal neurons in adult mice living in an enriched environment. *Nature* 1997; 386:493-5.
20. van Praag H, Kempermann G, Gage FH. Running increases cell proliferation and neurogenesis in the adult mouse dentate gyrus. *Nat Neurosci* 1999; 2:266-70.
21. Ajami B, Bennett JL, Krieger C, Tetzlaff W, Rossi FM. Local self-renewal can sustain CNS microglia maintenance and function throughout adult life. *Nat Neurosci* 2007; 10:1538-43.
22. Mildner A, Schmidt H, Nitsche M, Merkler D, Hanisch UK, Mack M, et al. Microglia in the adult brain arise from Ly-6ChiCCR2+ monocytes only under defined host conditions. *Nat Neurosci* 2007; 10:1544-53.
23. Walton NM, Sutter BM, Laywell ED, Levkoff LH, Kearns SM, Marshall GP, 2nd, et al. Microglia instruct subventricular zone neurogenesis. *Glia* 2006; 54:815-25.
24. Ziv Y, Ron N, Butovsky O, Landa G, Sudai E, Greenberg N, et al. Immune cells contribute to the maintenance of neurogenesis and spatial learning abilities in adulthood. *Nat Neurosci* 2006; 9:268-75.

25. Bachstetter AD, Morganti JM, Jernberg J, Schlunk A, Mitchell SH, Brewster KW, et al. Fractalkine and CX3CR1 regulate hippocampal neurogenesis in adult and aged rats. *Neurobiol Aging* 2011; 32:2030-44.
26. Kohman RA, DeYoung EK, Bhattacharya TK, Peterson LN, Rhodes JS. Wheel running attenuates microglia proliferation and increases expression of a proneurogenic phenotype in the hippocampus of aged mice. *Brain Behav Immun* 2012; 26:803-10.
27. Sierra A, Encinas JM, Deudero JJ, Chancey JH, Enikolopov G, Overstreet-Wadiche LS, et al. Microglia shape adult hippocampal neurogenesis through apoptosis-coupled phagocytosis. *Cell Stem Cell* 2010; 7:483-95.
28. Vukovic J, Colditz MJ, Blackmore DG, Ruitenber MJ, Bartlett PF. Microglia modulate hippocampal neural precursor activity in response to exercise and aging. *J Neuroscience* 2012; 32:6435-43.
29. Gemma C, Bachstetter AD. The role of microglia in adult hippocampal neurogenesis. *Front Cell Neurosci* 2013; 7:229.
30. Jung S, Aliberti J, Graemmel P, Sunshine MJ, Kreutzberg GW, Sher A, et al. Analysis of fractalkine receptor CX3CR1 function by targeted deletion and green fluorescent protein reporter gene insertion. *Mol Cell Biol* 2000; 20:4106-14.
31. Chinnery HR, Humphries T, Clare A, Dixon AE, Howes K, Moran CB, et al. Turnover of bone marrow-derived cells in the irradiated mouse cornea. *Immunol* 2008; 125:541-8.
32. Guzman-Marin R, Suntsova N, Bashir T, Szymusiak R, McGinty D. Cell proliferation in the dentate gyrus of the adult rat fluctuates with the light-dark cycle. *Neurosci Lett* 2007; 422:198-201.
33. West MJ, Slomianka L, Gundersen HJ. Unbiased stereological estimation of the total number of neurons in the subdivisions of the rat hippocampus using the optical fractionator. *Anat Rec* 1991; 231:482-97.

34. Franklin KB, Paxinos G. The mouse brain in stereotaxic coordinates. 3rd ed. San Diego: Academic Press; 2007.
35. de Winter JC. Using the Student's t-test with extremely small sample sizes. *Prac Assess Res Eval* 2013; 18:1-2.
36. Monje ML, Mizumatsu S, Fike JR, Palmer TD. Irradiation induces neural precursor-cell dysfunction. *Nat Med* 2002; 8:955-62.
37. Tada E, Parent JM, Lowenstein DH, Fike JR. X-irradiation causes a prolonged reduction in cell proliferation in the dentate gyrus of adult rats. *Neurosci* 2000; 99:33-41.
38. Mizumatsu S, Monje ML, Morhardt DR, Rola R, Palmer TD, Fike JR. Extreme sensitivity of adult neurogenesis to low doses of X-irradiation. *Cancer Res* 2003; 63:4021-7.
39. Fike JR, Rosi S, Limoli CL. Neural precursor cells and central nervous system radiation sensitivity. *Semin Radiat Oncol* 2009; 19:122-32.
40. Hellstrom NA, Bjork-Eriksson T, Blomgren K, Kuhn HG. Differential recovery of neural stem cells in the subventricular zone and dentate gyrus after ionizing radiation. *Stem Cells* 2009; 27:634-41.
41. Ben Abdallah NM, Slomianka L, Lipp HP. Reversible effect of X-irradiation on proliferation, neurogenesis, and cell death in the dentate gyrus of adult mice. *Hippocampus* 2007; 17:1230-40.
42. van Praag H, Christie BR, Sejnowski TJ, Gage FH. Running enhances neurogenesis, learning, and long-term potentiation in mice. *Proc Natl Acad Sci USA* 1999; 96:13427-31.
43. Fan Y, Liu Z, Weinstein PR, Fike JR, Liu J. Environmental enrichment enhances neurogenesis and improves functional outcome after cranial irradiation. *Eur J Neurosci* 2007; 25:38-46.

44. Meshi D, Drew MR, Saxe M, Ansorge MS, David D, Santarelli L, et al. Hippocampal neurogenesis is not required for behavioral effects of environmental enrichment. *Nat Neurosci* 2006; 9:729-31.
45. Brown J, Cooper-Kuhn CM, Kempermann G, Van Praag H, Winkler J, Gage FH, et al. Enriched environment and physical activity stimulate hippocampal but not olfactory bulb neurogenesis. *Eur J Neurosci* 2003; 17:2042-6.
46. Olson AK, Eadie BD, Ernst C, Christie BR. Environmental enrichment and voluntary exercise massively increase neurogenesis in the adult hippocampus via dissociable pathways. *Hippocampus* 2006; 16:250-60.
47. Rhodes JS, van Praag H, Jeffrey S, Girard I, Mitchell GS, Garland T, Jr., et al. Exercise increases hippocampal neurogenesis to high levels but does not improve spatial learning in mice bred for increased voluntary wheel running. *Behav Neurosci* 2003; 117:1006-16.
48. Stranahan AM, Khalil D, Gould E. Social isolation delays the positive effects of running on adult neurogenesis. *Nat Neurosci* 2006; 9:526-33.
49. Leasure JL, Decker L. Social isolation prevents exercise-induced proliferation of hippocampal progenitor cells in female rats. *Hippocampus* 2009; 19:907-12.
50. Naylor AS, Persson AI, Eriksson PS, Jonsdottir IH, Thorlin T. Extended voluntary running inhibits exercise-induced adult hippocampal progenitor proliferation in the spontaneously hypertensive rat. *J Neurophysiol* 2005; 93:2406-14.
51. Williamson LL, Chao A, Bilbo SD. Environmental enrichment alters glial antigen expression and neuroimmune function in the adult rat hippocampus. *Brain Behav Immun* 2012; 26:500-10.
52. Olah M, Ping G, De Haas AH, Brouwer N, Meerlo P, Van Der Zee EA, et al. Enhanced hippocampal neurogenesis in the absence of microglia T cell interaction and microglia activation in the murine running wheel model. *Glia* 2009; 57:1046-61.

53. Simard AR, Rivest S. Bone marrow stem cells have the ability to populate the entire central nervous system into fully differentiated parenchymal microglia. *FASEB J* 2004; 18:998-1000.
54. Davoust N, Vuillat C, Androdias G, Nataf S. From bone marrow to microglia: barriers and avenues. *Trends Immunol* 2008; 29:227-34.
55. Acharya MM, Patel NH, Craver BM, Tran KK, Giedzinski E, Tseng BP, et al. Consequences of low dose ionizing radiation exposure on the hippocampal microenvironment. *PLoS One* 2015; 10:e0128316.
56. Morganti JM, Jopson TD, Liu S, Gupta N, Rosi S. Cranial irradiation alters the brain's microenvironment and permits CCR2+ macrophage infiltration. *PloS One* 2014; 9:e93650.
57. Bulloch K, Miller MM, Gal-Toth J, Milner TA, Gottfried-Blackmore A, Waters EM, et al. CD11c/EYFP transgene illuminates a discrete network of dendritic cells within the embryonic, neonatal, adult, and injured mouse brain. *J Comp Neurol* 2008; 508:687-710.
58. Spalding KL, Bergmann O, Alkass K, Bernard S, Salehpour M, Huttner HB, et al. Dynamics of hippocampal neurogenesis in adult humans. *Cell* 2013; 153:1219-27.
59. Monje ML, Vogel H, Masek M, Ligon KL, Fisher PG, Palmer TD. Impaired human hippocampal neurogenesis after treatment for central nervous system malignancies. *Ann Neurol* 2007; 62:515-20.
60. Clark PJ, Kohman RA, Miller DS, Bhattacharya TK, Brzezinska WJ, Rhodes JS. Genetic influences on exercise-induced adult hippocampal neurogenesis across 12 divergent mouse strains. *Genes Brain Behav* 2011; 10:345-53.
61. Overall RW, Walker TL, Leiter O, Lenke S, Ruhwald S, Kempermann G. Delayed and transient increase of adult hippocampal neurogenesis by physical exercise in DBA/2 mice. *PLoS One*. 2013; 8:e83797.

FIGURE LEGENDS

Figure 1: Experimental design and housing conditions. (A) Following an 8-week recovery period after irradiation, mice were placed in one of three experimental housing conditions for an additional 8-week period, during which BrdU injections were administered to label proliferating cells. Sedentary animals were housed in standard laboratory cages with nesting materials (n=8). Runners were housed in similar standard laboratory cages containing a running wheel with odometer attached (n=6). Enriched animals were housed in several cages interconnected by plastic tubing (n=8). The overall design increased in complexity and changed in orientation each week over the 8 weeks of the experiment. In week 1 the set-up consisted of cages, a running wheel and a separate food supply over two levels (B). In week 6 there were additional cages, a maze and increased tubing over five levels (C).

Figure 2. Cell proliferation in the hippocampus of non-irradiated and irradiated mice.

Representative photomicrographs of BrdU^{pos} cells in the dentate gyrus of naïve controls (i.e. age-matched non-irradiated Balb/C mice; A), and irradiated bone marrow chimeric mice (B-D) that were housed in standard laboratory cages (B), in environmental enrichment (C), or in standard cages with running wheel (D). Insets (upper right in photomicrograph) show a higher power image of BrdU^{pos} cells within the granule cell layer (boxed area). (E,F) Scatter plot showing total estimated BrdU^{pos} (E) and DCX^{pos} (F) cell numbers in the granule cell layer of individual mice for each of the experimental groups. Note that DCX^{pos} cell counts for the environmentally enriched condition were derived from just two mice, and this should be taken into account when interpreting these findings. One-way ANOVA, Tukey's *post-hoc*, *p<0.05; ***p<0.001; ****P<0.0001.

Figure 3. Quantitative analysis of Iba1^{POS} cells in the granule cell layer and the dentate gyrus of the hippocampus. (A) Representative image of the distribution of Iba1-stained cells in the dentate gyrus of mice that were housed under environmentally enriched conditions. (B) Enlargement of the boxed area in A, showing Iba1^{POS} microglia with typical ramified morphology, both within and close to the granule cell layer. (C, D) Scatter plots showing the total estimated Iba1^{POS} cell numbers in the granule cell layer and the entire dentate gyrus for individual mice under the various housing conditions. One-way ANOVA, Tukey's *post-hoc* * $p < 0.05$.

Figure 4. Influx of microglia precursor cells into the hippocampus of chimeric mice under different housing conditions. (A) Confocal photomicrographs of donor, bone marrow-derived cells (GFP^{POS} cells) in the hippocampus of chimeric mice at 16 weeks post-transplantation. Confocal z-stack images showing that ramified GFP^{POS} cells (green) co-stain with microglia marker Iba1 (red) (arrows). (B) Double immunofluorescent staining showing ramified (arrow) and elongated (open arrows) GFP^{POS} cells (green) in relation to pan-laminin expression (red). Note that pan-laminin immunoreactivity in vascular structures is co-extensive with the elongated but not ramified GFP^{POS} cells. Hoechst-3 labelled nuclei are shown in blue. (C) Donor bone marrow-derived cells were immunohistochemically stained for GFP (brown). Few GFP^{POS} cells were encountered in the dorsal (green box) aspect of the dentate gyrus; ventral dentate gyrus indicated by a purple box (D). A greater number of GFP^{POS} cells was observed in the ventral dentate gyrus (E). (F) Schematic diagram illustrating the anatomy of the hippocampus at -1.94 mm (*top left*) and -2.92 mm (*right*) from Bregma. The arrow and arrowhead signify the dorsal and ventral part of the dentate gyrus, respectively. (G) Estimated GFP^{POS} cell numbers for the entire hippocampal formation (Hipp), dentate gyrus (DG) and anatomical sub-regions. Note the differences in spatial distribution of donor

BM-derived microglia between the dorsal and ventral subregions of the hippocampus ($p < 0.0001$, repeated measures two-way ANOVA). Housing conditions did not influence the number of GFP^{pos} (i.e., infiltrated) cells ($n = 5$ per experimental group; repeated measures two-way ANOVA, $p > 0.05$). Abbreviations: GrDG, granule cell layer of the dentate gyrus; PoDG, polymorph layer of the dentate gyrus; MoDG, molecular layer of the dentate gyrus; Or, oriens layer of the hippocampus; Py, pyramidal cell layer of the dentate gyrus; Rad, radiatum layer of the hippocampus; LMol, lacunosum moleculare layer of the hippocampus.

Fig.1

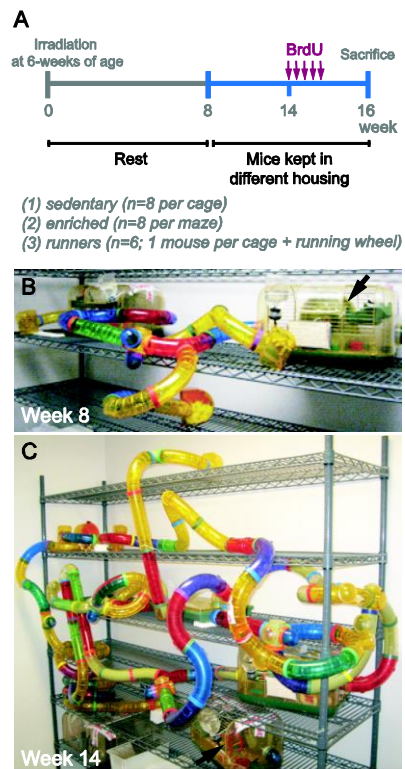


Figure 1

Fig.2

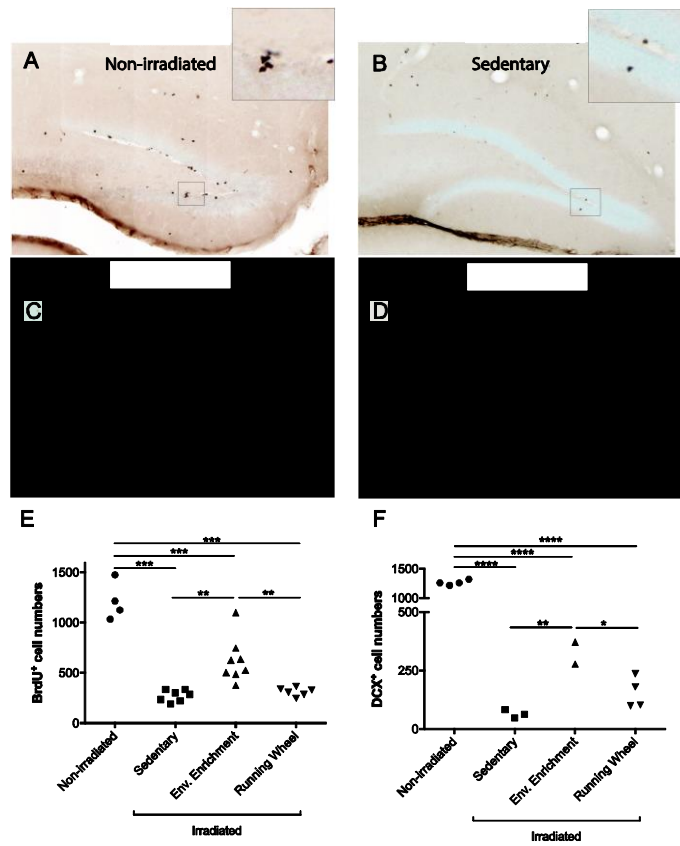


Figure 2

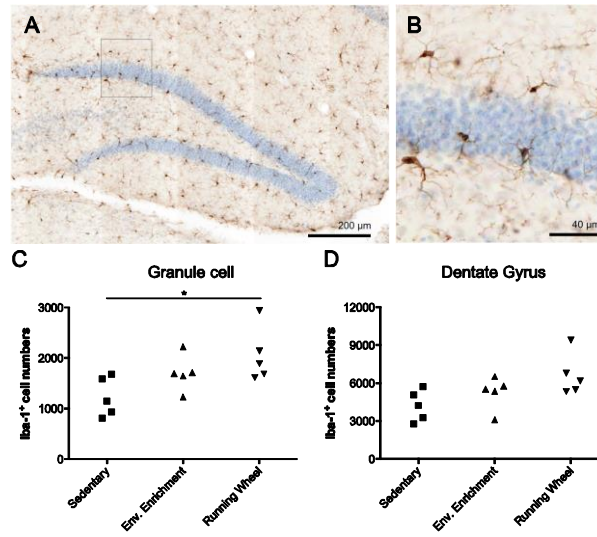


Figure 3

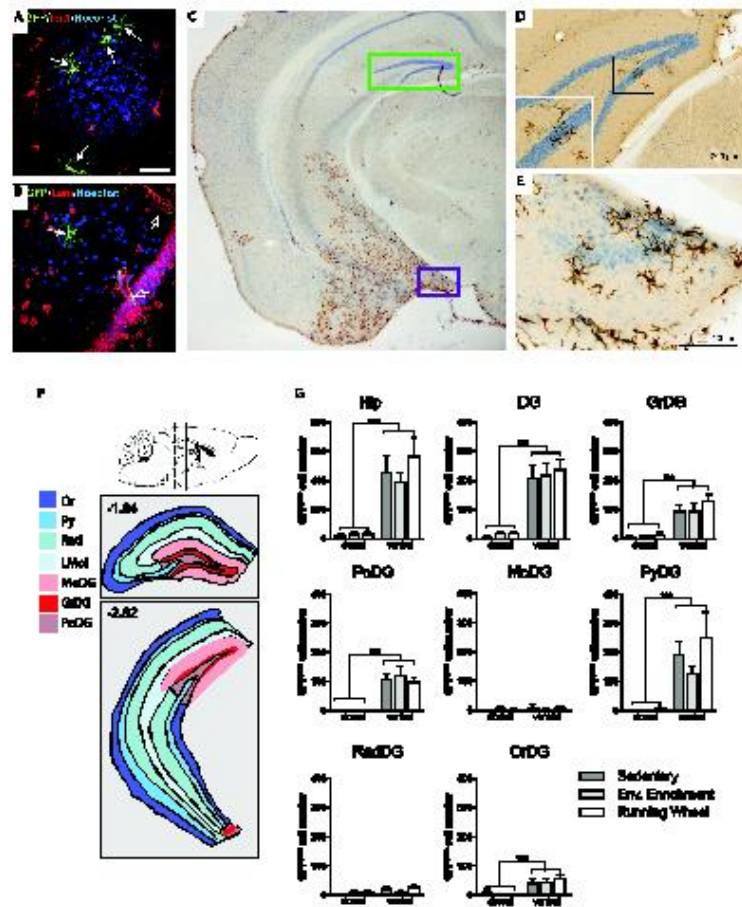


Figure 4

Table 1. BM-derived *Cx3cr1^{+gfp}* cell numbers in sub-regions of the hippocampus (Mean \pm SEM)

Structure		Sedentary	Env. Enrichment	Running Wheel
Hipp.	Dorsal	20 \pm 15	30 \pm 12	31 \pm 10
	Ventral	454 \pm 115	395 \pm 58	565 \pm 129
DG	Dorsal	7 \pm 4	16 \pm 8	16 \pm 8
	Ventral	206 \pm 46	217 \pm 43	235 \pm 38
GrDG	Dorsal	6 \pm 3	8 \pm 5	13 \pm 8
	Ventral	93 \pm 23	94 \pm 28	130 \pm 28
PoDG	Dorsal	1 \pm 1	2 \pm 1	0 \pm 0
	Ventral	104 \pm 24	120 \pm 29	97 \pm 16
MoDG	Dorsal	0 \pm 0	6 \pm 5	3 \pm 2
	Ventral	9 \pm 9	3 \pm 2	9 \pm 6
Py	Dorsal	2 \pm 2	2 \pm 1	5 \pm 4
	Ventral	189 \pm 47	126 \pm 23	249 \pm 89
Rad	Dorsal	0 \pm 0	9 \pm 5	8 \pm 7
	Ventral	19 \pm 12	7 \pm 6	26 \pm 10
Or	Dorsal	10 \pm 10	2 \pm 2	1 \pm 1
	Ventral	41 \pm 16	44 \pm 12	56 \pm 14